Observing Application

Date:	Aug 01, 2018
Proposal ID:	GBT/19A-347
Legacy ID:	QO43
PI:	Trevor Oxholm
Type:	Regular
Category:	Normal Galaxies, Groups, and Clusters
Total time:	6.24

Calibration sources for the Tianlai 21 cm Polar Cap Survey

Abstract:

We request observing time with two different GBT receivers to calibrate 67 radio sources for use as calibrators for a 21-cm intensity-mapping survey with a new instrument -- the Tianlai Dish Array. Specifically, we request a total of three hours to calibrate these sources in the 700--800~MHz band with the GBT PF1 (0.68 - 0.92 GHz) receiver, and three hours in the 1170--1270~MHz band with the GBT L (1.15 ? 1.73 GHz) receiver. To our knowledge, these sources have not been calibrated in these bands before. We request two observing sessions with each receiver, for a total of 4 observing sessions and a total of six hours of observing time.

Authors:

Name	Institution	Email	Status
Oxholm, Trevor	Wisconsin at Madison, University of	oxholm@wisc.edu	Graduating: N/A Thesis: true
Timbie, Peter	Wisconsin at Madison, University of	pttimbie@wisc.edu	

Principal Investigator:	Trevor Oxholm
Contact:	Trevor Oxholm
Telephone:	8603035100
Email:	oxholm@wisc.edu

Related Proposals:

Joint:

Not a Joint Proposal.

Observing type(s):

Single Pointing(s)

GBT Resources

Name	Group	Frontend & Backend	Setup
750MHz	750_MHz	PF1 800 MHz (0.680-0.920 GHz) VEGAS	Observing type: Spectral Line Number of beams: 1 Number of spectrometers: 1

Name	Group	Frontend & Backend	Setup

Spectrometer #	1
Mode	7
Bandwidth (MHz)	100.0
Rest frequences (GHz)	.750
Spectral resolution (KHz)	3.1
Integration time (s)	60.0
Data rate (MB/s)	0.0083

Name	Group	Frontend & Backend	Setup
1220MHz	1220_MHz	L-Band (1.15-1.73 GHz) VEGAS	Observing type: Spectral Line Number of beams: 1 Number of spectrometers: 1

Spectrometer #	1
Mode	7
Bandwidth (MHz)	100.0
Rest frequences (GHz)	1.220
Spectral resolution (KHz)	3.1
Integration time (s)	60.0
Data rate (MB/s)	0.0083

Sources

Name	Position		Velocity		Group
region4_1	**Coordinate system**	Equatorial	**Convention**	Radio	grp1
	Equinox	J2000			
	Right Ascension	16:25:57.0	**Ref. frame**	Barycentric	
		00:00:00			
	Declination	+41:34:41.0	**Velocity**	0	
		00:00:00			
	Calibrator	No			
region4_2	**Coordinate system**	Equatorial	**Convention**	Radio	grp1
	Equinox	J2000			
	Right Ascension	16:28:38.0	**Ref. frame**	Barycentric	
		00:00:00			
	Declination	+39:32:59.0	**Velocity**	0	
		00:00:00			
	Calibrator	No			

Name	Position		Velocity		Group
region4_3	**Coordinate system**	Equatorial	**Convention**	Radio	grp1
	Equinox	J2000			
	Right Ascension	16:28:53.0	**Ref. frame**	Barycentric	
		00:00:00			
	Declination	+44:19:05.0	**Velocity**	0	
		00:00:00			
	Calibrator	No			
region4_4	**Coordinate system**	Equatorial	**Convention**	Radio	grp1
	Equinox	J2000			
	Right Ascension	16:31:13.0	**Ref. frame**	Barycentric	
		00:00:00			
	Declination	+43:48:39.0	**Velocity**	0	
		00:00:00			
	Calibrator	No			
region4_5	**Coordinate system**	Equatorial	**Convention**	Radio	grp1
	Equinox	J2000			
	Right Ascension	16:34:02.0	**Ref. frame**	Barycentric	
		00:00:00			
	Declination	+39:00:00.0	**Velocity**	0	
		00:00:00			
	Calibrator	No			
region4_6	**Coordinate system**	Equatorial	**Convention**	Radio	grp1
	Equinox	J2000			
	Right Ascension	16:35:02.0	**Ref. frame**	Barycentric	
		00:00:00			
	Declination	+37:22:18.0	**Velocity**	0	
		00:00:00			
	Calibrator	No			
region4_7	**Coordinate system**	Equatorial	**Convention**	Radio	grp1
	Equinox	J2000			
	Right Ascension	16:35:15.0	**Ref. frame**	Barycentric	
		00:00:00			
	Declination	+38:08:04.0	**Velocity**	0	
		00:00:00			
	Calibrator	No			
region4_8	**Coordinate system**	Equatorial	**Convention**	Radio	grp1
	Equinox	J2000			
	Right Ascension	16:38:04.0	**Ref. frame**	Barycentric	
		00:00:00			
	Declination	+37:53:07.0	**Velocity**	0	
		00:00:00			
	Calibrator	No			

Name	Position		Velocity		Group
region4_9	Coordinate system	Equatorial	Convention	Radio	grp1
	Equinox	J2000			
	Right Ascension	16:38:46.0	Ref. frame	Barycentric	
		00:00:00			
	Declination	+42:33:36.0	Velocity	0	
		00:00:00			
	Calibrator	No			
region4_10	Coordinate system	Equatorial	Convention	Radio	grp1
	Equinox	J2000			
	Right Ascension	16:40:29.0	Ref. frame	Barycentric	
		00:00:00			
	Declination	+39:46:46.0	Velocity	0	
		00:00:00			
	Calibrator	No			
region4_11	Coordinate system	Equatorial	Convention	Radio	grp1
	Equinox	J2000			
	Right Ascension	16:40:32.0	Ref. frame	Barycentric	
		00:00:00			
	Declination	+38:26:41.0	Velocity	0	
		00:00:00			
	Calibrator	No			
region4_12	Coordinate system	Equatorial	Convention	Radio	grp1
	Equinox	J2000			
	Right Ascension	16:41:19.0	Ref. frame	Barycentric	
		00:00:00			
	Declination	+38:02:47.0	Velocity	0	
		00:00:00			
	Calibrator	No			
region4_13	Coordinate system	Equatorial	Convention	Radio	grp1
	Equinox	J2000			
	Right Ascension	16:41:30.0	Ref. frame	Barycentric	
		00:00:00			
	Declination	+42:09:25.0	Velocity	0	
		00:00:00			
	Calibrator	No			
3C_345	Coordinate system	Equatorial	Convention	Radio	grp1
	Equinox	J2000			
	Right Ascension	16:42:58.0	Ref. frame	Barycentric	
		00:00:00			
	Declination	+39:48:37.0	Velocity	0	
		00:00:00			
	Calibrator	No			

Name	Position		Velocity		Group
region4_14	**Coordinate system**	Equatorial	**Convention**	Radio	grp1
	Equinox	J2000			
	Right Ascension	16:43:05.0	**Ref. frame**	Barycentric	
		00:00:00			
	Declination	+37:29:34.0	**Velocity**	0	
		00:00:00			
	Calibrator	No			
region4_15	**Coordinate system**	Equatorial	**Convention**	Radio	grp1
	Equinox	J2000			
	Right Ascension	16:45:02.0	**Ref. frame**	Barycentric	
		00:00:00			
	Declination	+40:10:36.0	**Velocity**	0	
		00:00:00			
	Calibrator	No			
region4_16	**Coordinate system**	Equatorial	**Convention**	Radio	grp1
	Equinox	J2000			
	Right Ascension	16:46:05.0	**Ref. frame**	Barycentric	
		00:00:00			
	Declination	+37:12:31.0	**Velocity**	0	
		00:00:00			
	Calibrator	No			
region4_17	**Coordinate system**	Equatorial	**Convention**	Radio	grp1
	Equinox	J2000			
	Right Ascension	16:46:28.0	**Ref. frame**	Barycentric	
		00:00:00			
	Declination	+38:31:13.0	**Velocity**	0	
		00:00:00			
	Calibrator	No			
region4_18	**Coordinate system**	Equatorial	**Convention**	Radio	grp1
	Equinox	J2000			
	Right Ascension	16:46:56.0	**Ref. frame**	Barycentric	
		00:00:00			
	Declination	+40:59:17.0	**Velocity**	0	
		00:00:00			
	Calibrator	No			
region4_19	**Coordinate system**	Equatorial	**Convention**	Radio	grp1
	Equinox	J2000			
	Right Ascension	16:47:25.0	**Ref. frame**	Barycentric	
		00:00:00			
	Declination	+37:52:18.0	**Velocity**	0	
		00:00:00			
	Calibrator	No			

Name	Position		Velocity		Group
region4_20	Coordinate system	Equatorial	Convention	Radio	grp1
	Equinox	J2000			
	Right Ascension	16:48:00.0	Ref. frame	Barycentric	
		00:00:00			
	Declination	+37:44:29.0	Velocity	0	
		00:00:00			
	Calibrator	No			
region4_21	Coordinate system	Equatorial	Convention	Radio	grp1
	Equinox	J2000			
	Right Ascension	16:48:06.0	Ref. frame	Barycentric	
		00:00:00			
	Declination	+38:01:05.0	Velocity	0	
		00:00:00			
	Calibrator	No			
region4_22	Coordinate system	Equatorial	Convention	Radio	grp1
	Equinox	J2000			
	Right Ascension	16:48:29.0	Ref. frame	Barycentric	
		00:00:00			
	Declination	+41:04:05.0	Velocity	0	
		00:00:00			
	Calibrator	No			
region4_23	Coordinate system	Equatorial	Convention	Radio	grp1
	Equinox	J2000			
	Right Ascension	16:48:42.0	Ref. frame	Barycentric	
		00:00:00			
	Declination	+42:40:25.0	Velocity	0	
		00:00:00			
	Calibrator	No			
region4_24	Coordinate system	Equatorial	Convention	Radio	grp1
	Equinox	J2000			
	Right Ascension	16:48:49.0	Ref. frame	Barycentric	
		00:00:00			
	Declination	+38:48:14.0	Velocity	0	
		00:00:00			
	Calibrator	No			
region4_25	Coordinate system	Equatorial	Convention	Radio	grp1
	Equinox	J2000			
	Right Ascension	16:48:54.0	Ref. frame	Barycentric	
		00:00:00			
	Declination	+42:54:00.0	Velocity	0	
		00:00:00			
	Calibrator	No			

Name	Position		Velocity		Group
region4_26	**Coordinate system**	Equatorial	**Convention**	Radio	grp1
	Equinox	J2000			
	Right Ascension	16:53:52.0	**Ref. frame**	Barycentric	
		00:00:00			
	Declination	+39:45:36.0	**Velocity**	0	
		00:00:00			
	Calibrator	No			
region4_27	**Coordinate system**	Equatorial	**Convention**	Radio	grp1
	Equinox	J2000			
	Right Ascension	16:54:35.0	**Ref. frame**	Barycentric	
		00:00:00			
	Declination	+39:05:59.0	**Velocity**	0	
		00:00:00			
	Calibrator	No			
region4_28	**Coordinate system**	Equatorial	**Convention**	Radio	grp1
	Equinox	J2000			
	Right Ascension	16:58:22.0	**Ref. frame**	Barycentric	
		00:00:00			
	Declination	+39:06:25.0	**Velocity**	0	
		00:00:00			
	Calibrator	No			
NP_1	**Coordinate system**	Equatorial	**Convention**	Radio	grp1
	Equinox	J2000			
	Right Ascension	00:12:36.0	**Ref. frame**	Barycentric	
		00:00:00			
	Declination	+85:43:13.0	**Velocity**	0	
		00:00:00			
	Calibrator	No			
NP_2	**Coordinate system**	Equatorial	**Convention**	Radio	grp1
	Equinox	J2000			
	Right Ascension	01:10:45.0	**Ref. frame**	Barycentric	
		00:00:00			
	Declination	+87:38:22.0	**Velocity**	0	
		00:00:00			
	Calibrator	No			
NP_3	**Coordinate system**	Equatorial	**Convention**	Radio	grp1
	Equinox	J2000			
	Right Ascension	01:17:32.0	**Ref. frame**	Barycentric	
		00:00:00			
	Declination	+89:28:48.0	**Velocity**	0	
		00:00:00			
	Calibrator	No			

Name	Coordinate system	Equinox	Right Ascension	Declination	Calibrator	Convention	Ref. frame	Velocity	Group
NVSS_J022235+861727	Equatorial	J2000	02:22:35.0 00:00:00	+86:17:27.0 00:00:00	No	Radio	Barycentric	0	grp1
NVSS_J022248+861851	Equatorial	J2000	02:22:48.0 00:00:00	+86:18:51.0 00:00:00	No	Radio	Barycentric	0	grp1
NP_4	Equatorial	J2000	06:22:05.0 00:00:00	+87:19:48.0 00:00:00	No	Radio	Barycentric	0	grp1
NP_5	Equatorial	J2000	09:20:16.0 00:00:00	+86:28:45.0 00:00:00	No	Radio	Barycentric	0	grp1
NP_6	Equatorial	J2000	13:08:11.0 00:00:00	+85:44:24.0 00:00:00	No	Radio	Barycentric	0	grp1
NP_7	Equatorial	J2000	16:19:40.0 00:00:00	+85:49:21.0 00:00:00	No	Radio	Barycentric	0	grp1

Name	Position		Velocity		Group
NP_8	**Coordinate system**	Equatorial	**Convention**	Radio	grp1
	Equinox	J2000			
	Right Ascension	16:39:25.0	**Ref. frame**	Barycentric	
		00:00:00			
	Declination	+86:31:54.0	**Velocity**	0	
		00:00:00			
	Calibrator	No			
NP_9	**Coordinate system**	Equatorial	**Convention**	Radio	grp1
	Equinox	J2000			
	Right Ascension	18:37:12.0	**Ref. frame**	Barycentric	
		00:00:00			
	Declination	+85:14:49.0	**Velocity**	0	
		00:00:00			
	Calibrator	No			
NP_10	**Coordinate system**	Equatorial	**Convention**	Radio	grp1
	Equinox	J2000			
	Right Ascension	19:03:50.0	**Ref. frame**	Barycentric	
		00:00:00			
	Declination	+85:36:47.0	**Velocity**	0	
		00:00:00			
	Calibrator	No			
NP_11	**Coordinate system**	Equatorial	**Convention**	Radio	grp1
	Equinox	J2000			
	Right Ascension	19:41:36.0	**Ref. frame**	Barycentric	
		00:00:00			
	Declination	+85:01:38.0	**Velocity**	0	
		00:00:00			
	Calibrator	No			
NP_12	**Coordinate system**	Equatorial	**Convention**	Radio	grp1
	Equinox	J2000			
	Right Ascension	22:47:14.0	**Ref. frame**	Barycentric	
		00:00:00			
	Declination	+85:55:42.0	**Velocity**	0	
		00:00:00			
	Calibrator	No			
CygA	**Coordinate system**	Equatorial	**Convention**	Radio	grp1
	Equinox	J2000			
	Right Ascension	19:59:28.0	**Ref. frame**	Barycentric	
		00:00:00			
	Declination	+40:44:02.0	**Velocity**	0	
		00:00:00			
	Calibrator	No			

Name	Position		Velocity		Group
region2_1	**Coordinate system**	Equatorial	**Convention**	Radio	grp2
	Equinox	J2000			
	Right Ascension	03:12:26.0	**Ref. frame**	Barycentric	
		00:00:00			
	Declination	+39:16:30.0	**Velocity**	0	
		00:00:00			
	Calibrator	No			
region2_2	**Coordinate system**	Equatorial	**Convention**	Radio	grp2
	Equinox	J2000			
	Right Ascension	03:14:43.0	**Ref. frame**	Barycentric	
		00:00:00			
	Declination	+43:14:04.0	**Velocity**	0	
		00:00:00			
	Calibrator	No			
region2_3	**Coordinate system**	Equatorial	**Convention**	Radio	grp2
	Equinox	J2000			
	Right Ascension	03:18:16.0	**Ref. frame**	Barycentric	
		00:00:00			
	Declination	+41:54:17.0	**Velocity**	0	
		00:00:00			
	Calibrator	No			
region2_4	**Coordinate system**	Equatorial	**Convention**	Radio	grp2
	Equinox	J2000			
	Right Ascension	03:26:40.0	**Ref. frame**	Barycentric	
		00:00:00			
	Declination	+41:51:32.0	**Velocity**	0	
		00:00:00			
	Calibrator	No			
region2_5	**Coordinate system**	Equatorial	**Convention**	Radio	grp2
	Equinox	J2000			
	Right Ascension	03:30:27.0	**Ref. frame**	Barycentric	
		00:00:00			
	Declination	+41:01:42.0	**Velocity**	0	
		00:00:00			
	Calibrator	No			
region3_1	**Coordinate system**	Equatorial	**Convention**	Radio	grp2
	Equinox	J2000			
	Right Ascension	04:08:04.0	**Ref. frame**	Barycentric	
		00:00:00			
	Declination	+42:59:57.0	**Velocity**	0	
		00:00:00			
	Calibrator	No			

Name	Position		Velocity		Group
NVSS_J041815+380049	**Coordinate system**	Equatorial	**Convention**	Radio	grp2
	Equinox	J2000			
	Right Ascension	04:18:15.0	**Ref. frame**	Barycentric	
		00:00:00			
	Declination	+38:00:49.0	**Velocity**	0	
		00:00:00			
	Calibrator	No			
region3_2	**Coordinate system**	Equatorial	**Convention**	Radio	grp2
	Equinox	J2000			
	Right Ascension	04:20:13.0	**Ref. frame**	Barycentric	
		00:00:00			
	Declination	+38:49:43.0	**Velocity**	0	
		00:00:00			
	Calibrator	No			
region3_3	**Coordinate system**	Equatorial	**Convention**	Radio	grp2
	Equinox	J2000			
	Right Ascension	04:23:18.0	**Ref. frame**	Barycentric	
		00:00:00			
	Declination	+40:53:33.0	**Velocity**	0	
		00:00:00			
	Calibrator	No			
region3_4	**Coordinate system**	Equatorial	**Convention**	Radio	grp2
	Equinox	J2000			
	Right Ascension	04:23:30.0	**Ref. frame**	Barycentric	
		00:00:00			
	Declination	+43:30:35.0	**Velocity**	0	
		00:00:00			
	Calibrator	No			
region3_5	**Coordinate system**	Equatorial	**Convention**	Radio	grp2
	Equinox	J2000			
	Right Ascension	04:23:44.0	**Ref. frame**	Barycentric	
		00:00:00			
	Declination	+40:04:36.0	**Velocity**	0	
		00:00:00			
	Calibrator	No			
region3_6	**Coordinate system**	Equatorial	**Convention**	Radio	grp2
	Equinox	J2000			
	Right Ascension	04:23:55.0	**Ref. frame**	Barycentric	
		00:00:00			
	Declination	+41:50:03.0	**Velocity**	0	
		00:00:00			
	Calibrator	No			

Name	Position			Velocity		Group
region3_7	**Coordinate system**	Equatorial		**Convention**	Radio	grp2
	Equinox	J2000				
	Right Ascension	04:26:04.0	00:00:00	**Ref. frame**	Barycentric	
	Declination	+41:26:54.0	00:00:00	**Velocity**	0	
	Calibrator	No				
region3_8	**Coordinate system**	Equatorial		**Convention**	Radio	grp2
	Equinox	J2000				
	Right Ascension	04:27:46.0	00:00:00	**Ref. frame**	Barycentric	
	Declination	+41:33:00.0	00:00:00	**Velocity**	0	
	Calibrator	No				
region3_9	**Coordinate system**	Equatorial		**Convention**	Radio	grp2
	Equinox	J2000				
	Right Ascension	04:29:16.0	00:00:00	**Ref. frame**	Barycentric	
	Declination	+42:31:48.0	00:00:00	**Velocity**	0	
	Calibrator	No				
region3_10	**Coordinate system**	Equatorial		**Convention**	Radio	grp2
	Equinox	J2000				
	Right Ascension	04:31:46.0	00:00:00	**Ref. frame**	Barycentric	
	Declination	+44:41:47.0	00:00:00	**Velocity**	0	
	Calibrator	No				
region3_11	**Coordinate system**	Equatorial		**Convention**	Radio	grp2
	Equinox	J2000				
	Right Ascension	04:32:36.0	00:00:00	**Ref. frame**	Barycentric	
	Declination	+41:38:29.0	00:00:00	**Velocity**	0	
	Calibrator	No				
region3_12	**Coordinate system**	Equatorial		**Convention**	Radio	grp2
	Equinox	J2000				
	Right Ascension	04:36:11.0	00:00:00	**Ref. frame**	Barycentric	
	Declination	+39:02:52.0	00:00:00	**Velocity**	0	
	Calibrator	No				

Name	Position		Velocity		Group
region3_13	Coordinate system	Equatorial	Convention	Radio	grp2
	Equinox	J2000			
	Right Ascension	04:40:07.0	Ref. frame	Barycentric	
		00:00:00			
	Declination	+42:44:40.0	Velocity	0	
		00:00:00			
	Calibrator	No			
region3_14	Coordinate system	Equatorial	Convention	Radio	grp2
	Equinox	J2000			
	Right Ascension	04:46:17.0	Ref. frame	Barycentric	
		00:00:00			
	Declination	+39:45:02.0	Velocity	0	
		00:00:00			
	Calibrator	No			
region3_15	Coordinate system	Equatorial	Convention	Radio	grp2
	Equinox	J2000			
	Right Ascension	04:49:03.0	Ref. frame	Barycentric	
		00:00:00			
	Declination	+45:01:36.0	Velocity	0	
		00:00:00			
	Calibrator	No			
region3_16	Coordinate system	Equatorial	Convention	Radio	grp2
	Equinox	J2000			
	Right Ascension	04:49:33.0	Ref. frame	Barycentric	
		00:00:00			
	Declination	+42:17:47.0	Velocity	0	
		00:00:00			
	Calibrator	No			

Sessions:

Name	Session time (hours)	Repeat	Separation	LST minimum	LST maximum	Elevation minimum
session1	1.12	1	0 day	21:52:59	10:23:56	30
session2	2.0	1	0 day	11:39:22	21:51:42	30
session3	1.12	1	0 day	21:52:59	10:23:56	30
session4	2.0	1	0 day	11:39:22	21:51:42	30

Session Constraints:

Name	Scheduling constraints	Comments
session1	nighttime preferred	
session2	nighttime preferred	Min. elevation is flexible, though a higher elevation is preferred to reduce RFI potential

Name	Scheduling constraints	Comments
session3	nighttime preferred	Min. elevation is flexible, though a higher elevation is preferred to reduce RFI potential
session4	nighttime preferred	Min. elevation is flexible, though a higher elevation is preferred to reduce RFI potential

Session Source/Resource Pairs:

Session name	Source	Resource	Time
session1	region2_1 region2_2 region2_3 region2_4 region2_5 region3_1 NVSS_J041815+380049 region3_2 region3_3 region3_4 region3_5 region3_6 region3_7 region3_8 region3_9 region3_10 region3_11 region3_12 region3_13 region3_14 region3_15 region3_16	750MHz	1.12 hour
session2	region4_7 region4_8 region4_9 region4_10 region4_11 region4_12 region4_13 3C_345 region4_14 region4_15 region4_16 region4_17 region4_18 region4_19 region4_20 region4_21 region4_22 region4_23 region4_24 region4_25 region4_26 region4_27	750MHz	2.0 hour

Session name	Source	Resource	Time
	region4_28 NP_1 NP_2 NP_3 NVSS_J022235+861727 NVSS_J022248+861851 NP_4 NP_5 NP_6 NP_7 NP_8 NP_9 NP_10 NP_11 NP_12 region4_1 region4_2 region4_3 region4_4 region4_5 region4_6		
session3	region2_1 region2_2 region2_3 region2_4 region2_5 region3_1 NVSS_J041815+380049 region3_2 region3_3 region3_4 region3_5 region3_6 region3_7 region3_8 region3_9 region3_10 region3_11 region3_12 region3_13 region3_14 region3_15 region3_16	1220MHz	1.12 hour
session4	region4_7 region4_8 region4_9 region4_10 region4_11 region4_12 region4_13 3C_345 region4_14 region4_15 region4_16	1220MHz	2.0 hour

Session name	Source	Resource	Time
	region4_17 region4_18 region4_19 region4_20 region4_21 region4_22 region4_23 region4_24 region4_25 region4_26 region4_27 region4_28 NP_1 NP_2 NP_3 NVSS_J022235+861727 NVSS_J022248+861851 NP_4 NP_5 NP_6 NP_7 NP_8 NP_9 NP_10 NP_11 NP_12 region4_1 region4_2 region4_3 region4_4 region4_5 region4_6		

Present for observation: no Staff support: None Plan of dissertation: yes

Technical Justification:

Dates:

N/A

Observing time:

We will be performing four sessions with two different resources. The two sessions differ only in the receiver used. Spectral Line mode is used in both resource groups to allow us to analyze the raw data and observe any potential RFI.

For all sessions:
Backend: VEGAS
Mode: Spectral Line
Switching Mode: Position Switching
Polarization: Dual
Bandwidth: 100 MHz
Frequency resolution: varies
Receivers: PF1 (.69-.92 GHz), L (1.15-1.73 GHz)
On+off observing time: 60 seconds
Ratio of on / off position for reference observation: 1

Number of reference observations: 4
Frequency smoothing: .2 MHz

Sample output from sensitivity calculator for one source with 40 degree declination and 6K source contribution to system temperature:
Derived Sensitivity (1-sigma): 5.817555 mJy
Time at Siginal Position or Frequency: 30.00 s
Time at Reference Position or Frequency: 30.00 s
Effective Integration Time: 15.00 s
Obs. Mode Time Mult. Factor: 1
FWHM Beamwidth: 16.43 '
Aperture Efficiency: 0.70
Extended Source Efficiency: 0.70
Confusion Limit: 340.84 S (mJy)
Hrs Above Min Elevation: 9.19 hours
Topocentric Frequency: 750.000 MHz
Min. Topocentric Channel Width: 0.763 kHz
Desired Freq. or Vel. Resolution: 0.200000 MHz or km/s
Typical Air Mass: 1.2
Typical Atmospheric Attenuation: 1.008
Typical System Temperature: 19.9 K
Backend Sampling Efficiency (K1): 1.0000
Backend Channel Weighting (K2): 1.0000

Mapping:

N/A

RFI considerations:

RFI is potentially impactful for all four sessions. Because of this, we request nighttime observations with higher elevation. We observe in spectral line mode in order to identify and remove RFI. We will use the off-line data analysis code that we have developed for the Tianlai dish array analysis. Furthermore, we map each source for one minute, which is longer than necessary for our desired precision, to allow for additional buffer in the case of RFI.

Overhead:

Slew times were calculated by comparing the slew rates listed in the proposer's guide to a conservative 1 minute repointing time between sources, and taking whichever is larger. We also included 10 min point/focus time and 6 min calibration time per session. Further details are included in the science justification document.
Session 1:
integration time: 23 min
slew + overhead time: 43 min

Session 2:
integration time: 44 min
slew + overhead time: 72 min

Session 3:
integration time: 23 min
slew + overhead time: 43 min

Session 4:
integration time: 44 min
slew + overhead time: 72 min

Joint considerations:

N/A

Novel considerations:

N/A

Pulsar considerations:

N/A

LST Range Justification:

N/A

Calibration sources for the Tianlai 21 cm Polar Cap Survey

(Dated: August 1, 2018)

We request observing time with two different GBT receivers to calibrate 67 radio sources for use as calibrators for a 21-cm intensity-mapping survey with a new instrument – the Tianlai Dish Array. Specifically, we request a total of 3 hours to calibrate these sources in the 700–800 MHz band with the GBT PF1 (0.68 - 0.92 GHz) receiver, and 3 hours in the 1170–1270 MHz band with the GBT L (1.15 1.73 GHz) receiver. To our knowledge, these sources have not been calibrated in these bands before. We request two observing sessions with each receiver, for a total of 4 observing sessions and a total of 6 hours of observing time.

21 CM INTENSITY MAPPING

The technique of 'intensity-mapping' with the 21 cm line of neutral hydrogen (HI) has developed over the past decade as a possible means to measure large-scale structure in the Universe in a relatively inexpensive way [1–5]. Traditionally, large-scale cosmic structure is measured with galaxy redshift surveys, a time-consuming process that requires detecting a large number of individual galaxies and determining their positions and redshifts. The fundamental idea behind 21 cm intensity-mapping is to measure the combined neutral hydrogen emission from many galaxies at once, simultaneously reducing the required angular resolution of the telescope and increasing the signal-to-noise ratio.

The most significant challenge to 21 cm intensity-mapping is extracting the HI signal from strong Galactic foregrounds that are $\sim$ 1000 times greater. In principle, the foregrounds should be separable from the signal because the spectra are very different: the foregrounds are dominated by synchrotron radiation and free-free emission, which have smooth, power-law spectra, while the HI signal from clumps of HI emitting at different redshifts forms a 'spikey' spectrum. In practice, instrumental effects introduce structure into the spectra. The first measurements of the HI power spectrum using 21 cm intensity-mapping, reported beginning in 2010, were made with the GBT at $z \sim 0.8$. To overcome systematic effects, HI maps were cross-correlated with maps of galaxy number counts from the DEEP2 and WiggleZ galaxy redshift surveys [4, 6–8]. The goal for future surveys is to detect the 21 cm signal directly, without cross-correlation with known structures.

To survey large swaths of the sky with adequate signal-to-noise requires dedicated instrumentation. Both single dish and interferometric approaches are being developed. Although single-dish instruments like the GBT may have less chromatic response than do interferometers, and hence have a significant advantage for the removal of foregrounds and instrumental effects, it has proved difficult to increase the mapping speed of single-dish instruments to compete with that of large-N interferometers. As a result, most 21 cm intensity-mapping instruments are interferometers [9–13] and include cylindrical reflectors (Pittsburgh CRT[14], CHIME[15], the Tianlai cylinder array[16]) as well as arrays of single dishes (Tianlai dish array and HIRAX[17]).

THE TIANLAI 21 CM POLAR CAP SURVEY

Over the last decade our team has been developing the Tianlai Dish Array, which is specifically designed for 21 cm intensity mapping. It consists of sixteen, 6 m diameter dish antennas located in a radio-quiet part of northwest China ($44°9'9.66''$ N $91°48'24.72''$ E). The dishes can be pointed electronically for testing, but for science surveys they operate in drift-scan mode. The receivers can be tuned to observe in bands of width 100 MHz in the range from 600 MHz to 1420 MHz ($1.36 > z > 0$). The dish array saw first light in 2016 and we are now commissioning the instrument.

The dish array's first science surveys will be of the North polar cap in two different frequency bands: $700 - 800$ MHz ($1.03 > z > 0.78$) and $1170 - 1270$ MHz ($0.21 > z > 0.12$). The low redshift survey will overlap with an existing photometric optical galaxy survey of the polar cap (NCCS [18]). We are attempting to commission a spectroscopic optical survey of the same region to obtain redshifts for this sample of galaxies. This optical survey will be used for a cross-correlation analysis with the Tianlai dish survey. The high redshift Tianlai dish survey will explore new territory, without the benefit of a corresponding optical survey. We would like to calibrate the polar cap survey at both frequencies with an uncertainty of $2 - 3\%$.

Restricting our observations to this limited region of the sky (the dishes have FWHM of $3.0°$ at 750 MHz and $1.8°$ at 1220 MHz) will allow us to integrate to the expected level of the 21 cm signal over several days. However, there are no bright radio sources in the polar cap, and, because the sky moves so slowly there, the relatively dim point sources

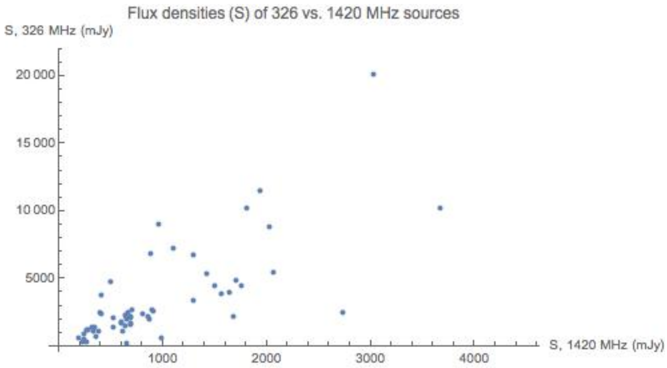

FIG. 1: Comparison between flux densities in 1420 MHz (NVSS) and 326 MHz (WENSS) surveys. While there is clearly a correlation between the two fluxes, the spread is too great to accurately extrapolate data from existing surveys to the frequencies of interest for the upcoming North Pole survey

in the field will modulate the observed visibilities very slowly. For these reasons the observations and calibration of the polar cap survey will occur in a two-step process for each of the two frequency bands.

Cygnus-A strip (DEC 40): First, before observing the polar cap itself, we will observe bright radio sources in a strip at the declination of Cygnus-A using a drift scan over a period of several days. Cygnus-A and other bright sources will allow us to measure the shape of the beams with high signal-to-noise and to study the stability of the calibration over periods from a few hours to 24 hours.

North Polar Cap (DEC 90): Second, we will observe the polar cap itself for a period of several days. We will use the brightest point sources in this field to calibrate the array in the course of the observations.

To our knowledge, the flux densities for the bright point sources in these two regions have not been measured in the 700-800 MHz or 1170-1270 MHz ranges of interest. They have been measured at 1420 MHz and 326 MHz by the NRAO VLA Sky Survey (NVSS) and the Westerbork Northern Sky Survey (WENSS), respectively. In order to find bright sources for the upcoming survey we extrapolated flux densities for sources based on a power law fit. However, a great deal of uncertainty is introduced through this extrapolation so a new survey is necessary to precisely measure sources in the 700-800 MHz and 1170-1270 MHz ranges.

We justify the need for a new survey with Figure 1. Here we compare flux densities at two different frequencies for a set of radio sources appearing in both the NVSS and WENSS surveys. The correlation between the fluxes at the two different frequencies is imperfect because each source follows a unique power law fit. We were able to roughly estimate the flux densities at the frequencies of interest, but a new measurement is necessary to reach the precision necessary for the Tianlai survey.

PROPOSED GBT OBSERVATIONS

We propose to observe a total of 67 sources located in 5 regions of the sky, each with two different receivers. We request 4 short (~ 1 hr each) observing sessions.

In the Cygnus-A (DEC 40) strip we have identified four compact regions that are dominated by a relatively small number of point sources. For each region we have identified the point sources that that will contribute more than 98% of the visibility signals in the Tianlai dish array. These regions are located near Dec 40° and 4 values of RA. In the region near Cygnus-A (RA 300°), Cygnus-A contributes this much signal by itself. Near RA 50° there are 6 sources, RA 65° has 17, and RA 250° has 29. In the polar cap region itself, there are 14 sources that dominate the expected visibilities in our two bands.

Each frequency band requires a different receiver. As justified below, we plan to use 60 second integration times for each source. This time will bring the uncertainty of Cygnus-A down to $\sim 0.07\%$, for both frequencies. Because Cygnus-A is the primary source for our study, it is important that we obtain a precise reading, with additional time to safeguard against RFI. Additionally, the other major sources at the declination of Cygnus-A will be known to the 0.1% level. The statistical errors on all polar cap sources will be better than 1%. These errors are below the absolute calibration error $(2-3\%)$ of our primary calibration source, Cygnus-A [19]. These errors correspond to knowing most sources within $\sim 1-10$ mJy. The integration time, including position switching from sources to reference fields, is 71 minutes for each receiver and 142 minutes for observations at both frequencies. The main sources in the five different

Source Name	**RA (deg)**	**DEC (deg)**	**S (750MHz) (mJy)**	**Precision (mJy)**	**S (1220MHz) (mJy)**	**Precision (mJy)**
Cygnus A	299.87	40.73	3000000	1558	850000	273
NGC 1275	49.95	41.51	33547.2	44.9	25608.9	22.9
NVSS J041815+380049	64.57	38.01	30433.0	41.8	18493.8	18
3C 345	250.74	39.81	8716.5	15.5	7547.3	9.8
NVSS J022235+861727	35.65	86.29	5233.8	7.7	2481.9	6.5
NVSS J022248+861851	35.70	86.31	6889.3	9.9	4430.3	7.8

TABLE I: Primary sources. In the region of each source, a number of other weaker sources are also being mapped. The flux densities S for each frequency are estimated based on extrapolations from the NVSS and WENSS surveys. Precisions for the proposed measurements were obtained by following the GBT sensitivity calculator with parameters described in Table II

Band	**Backend**	**Mode**	**Receiver**	**Polar-ization**	**Band-width**	**Switching Mode**	**Rest Frequency**	**Source Temp.**	**Resol-ution**
700 - 800 MHz	VEGAS	Spectral Line	PF1 (.68 - .92 GHz)	Dual	100 MHz	Position	750 MHz	varies	.2 MHz
1170 - 1270 MHz	VEGAS	Spectral Line	L (1.15 - 1.73 GHz)	Dual	100 MHz	Position	1220 MHz	varies	.2 MHz

TABLE II: Specifications for our proposed observations in two different frequency bands. Each source will be observed twice; once per frequency band.

regions are displayed in Table I.

TECHNICAL JUSTIFICATION

Sensitivity Calculations: We designed the calibration observations using the parameters shown in Table II. We tested the specifications for each of the 67 sources with the sensitivity calculator, each with a unique source contribution to system noise temperature, and found that the primary sources featured uncertainties well below the percent level. Additionally, we found that the anticipated errors on the primary sources are well above the confusion limit.

RFI: Although we ultimately require broad-band flux densities, we will observe in spectral line mode in order to identify and remove RFI. For this purpose we will use the off-line data analysis code that we have developed for the Tianlai dish array analysis. We prefer to observe at night, with higher elevation, in order to minimize RFI. Furthermore, we map each source for one minute, which is longer than necessary for our desired precision, to allow for additional buffer in the case of RFI.

Observing Sessions: The NCP targets are always visible to the GBT but only part of the Cygnus strip can be seen at any one time. We propose two observing sessions with each receiver, for a total of four sessions. For each receiver, one session would observe the two of the four regions on the Cygnus-A strip as well as the NCP region. A second session for each receiver would observe the other two regions of the Cygnus-A strip. In Table III we list the agenda for the 4 proposed observing sessions. We make the following assumptions about the time allocations for those sessions:

Slewing Time: Our sessions involve two types of slewing: slewing within regions, and slewing from one region to the next. Within regions, we conservatively estimate the time to move from one source to the next and to start a new integration to be 60 seconds. For slewing between regions, we use a slewing rate of 35.2 degrees/min and 17.6 degrees/min for azimuth and elevation, respectively. This results in slew times ranging from 30 seconds to 4 minutes.

Pointing and Focusing Time: Following the recommendation of the GBT Observer's Guide, we plan one pointing and focusing operation at the beginning of each observing session. We assume this process will take about 10 minutes. How about time for calibration before and after?

Calibration Time: After pointing a focusing, we will observe one bright, standard calibration source. Even when Cygnus-A is one of our targets, we propose to observe another calibrator as a test.

Overhead Time: We budget an overhead of at least 10% for each session.

Session	Receiver	DEC (deg)	RA (deg)	# Sources	integ	in-region slew	between-region slew	point/focus	cal	o'hd	Total
1	PF1	40	50	6	6 min	5 min	-	10 min	6 min	6 min	67 min
	680 - 920 MHz	40	65	17	17 min	16 min	1 min				
2	PF1	40	250	29	29 min	28 min	-	10 min	6 min	11 min	116 min
	680 - 920 MHz	40	300	1	1 min	0 min	1.5 min				
		90	-	14	14 min	13 min	3 min				
3	L	40	50	6	6 min	5 min	-	10 min	6 min	6 min	67 min
	1.15 1.73 GHz	40	65	17	17 min	16 min	1 min				
4	L	40	250	29	29 min	28 min	-	10 min	6 min	11 min	116 min
	1.15 1.73 GHz	40	300	1	1 min	0 min	1.5 min				
		90	-	14	14 min	13 min	3 min				

TABLE III: The agenda for each of the proposed 4 observing sessions. The DEC and RA refer to the rough location of the center of each region to be studied. The locations of the sources within each region at given in Table I. The integration time includes time both on and off source for position switching. In-region slew refers to the total time in a given (DEC,RA) region, while between-region slew is the time it takes to point from one region to the next.

STUDENT TRAINING

There are currently a number of graduate students working on the Tianlai program in the US, France, and China. One of them, Trevor Oxholm, is the PI of this proposal. He is starting his second year in the Ph.D. program in Physics at UW-Madison and is focusing on the North Polar Cap Survey for his first Ph.D. project. This will be his first use of the GBT but he is advised by experienced GBT users, including his thesis advisor, Co-I Peter Timbie.

CONCLUSION

Subtracting the strong foregrounds from the Tianlai polar cap survey requires exquisite knowledge of the response of the instrument: *i.e.* calibration. For this reason, we are requesting GBT observing time to calibrate bright sources in our observing bands in and near the North polar cap.

---

[1] F. B. Abdalla and S. Rawlings, MNRAS **360**, 27 (2005), astro-ph/0411342.
[2] J. B. Peterson, K. Bandura, and U. L. Pen, ArXiv Astrophysics e-prints (2006), astro-ph/0606104.
[3] M. F. Morales, in *The Evolution of Galaxies Through the Neutral Hydrogen Window*, edited by R. Minchin and E. Momjian (2008), vol. 1035 of *American Institute of Physics Conference Series*, pp. 82–86, 0810.5136.
[4] T.-C. Chang, U.-L. Pen, J. B. Peterson, and P. McDonald, Phys. Rev. Lett. **100** (2008).
[5] Y. Mao, M. Tegmark, M. McQuinn, M. Zaldarriaga, and O. Zahn, PRD **78**, 023529 (2008), 0802.1710.
[6] T. Chang, U. Pen, K. Bandura, and J. B. Peterson, Nature **466**, 463 (2010).
[7] K. W. Masui, E. R. Switzer, N. Banavar, K. Bandura, C. Blake, L.-M. Calin, T.-C. Chang, X. Chen, Y.-C. Li, Y.-W. Liao, et al., ApJL **763**, L20 (2013), 1208.0331.
[8] E. R. Switzer, K. W. Masui, K. Bandura, L.-M. Calin, T.-C. Chang, X.-L. Chen, Y.-C. Li, Y.-W. Liao, A. Natarajan, U.-L. Pen, et al., MNRAS **434**, L46 (2013), 1304.3712.
[9] R. Ansari, J. . Le Goff, C. Magneville, M. Moniez, N. Palanque-Delabrouille, J. Rich, V. Ruhlmann-Kleider, and C. Yèche, ArXiv e-prints (2008), 0807.3614.
[10] H. Seo, S. Dodelson, J. Marriner, D. Mcginnis, A. Stebbins, C. Stoughton, and A. Vallinotto, ApJ **721**, 164 (2010), 0910.5007.
[11] R. Ansari, J. Campagne, P. CoIom, J. Le Goff, C. Magneville, J. Martin, M. Moniez, J. Rich, and C. Yeche, Astronomy & Astrophysics **540**, A129 (2012), ISSN 0004-6361.
[12] Y. Xu, X. Wang, and X. Chen, ApJ **798**, 40 (2015), 1410.7794.
[13] P. Bull, P. G. Ferreira, P. Patel, and M. G. Santos, ApJ **803**, 21 (2015), 1405.1452.
[14] K. Bandura, Ph.D. thesis, Carnegie Mellon University (2011).
[15] K. Bandura, G. E. Addison, M. Amiri, J. R. Bond, D. Campbell-Wilson, L. Connor, J.-F. Cliche, G. Davis, M. Deng, N. Denman, et al., in *Ground-based and Airborne Telescopes V* (2014), vol. 9145 of *Proc. SPIE*, p. 914522, 1406.2288.
[16] X. Chen, International Journal of Modern Physics Conference Series **12**, 256 (2012), 1212.6278.
[17] L. B. Newburgh, K. Bandura, M. A. Bucher, T.-C. Chang, H. C. Chiang, J. F. Cliche, R. Dave, M. Dobbs, C. Clarkson, K. M. Ganga, et al., ArXiv e-prints (2016), 1607.02059.
[18] E. Gorbikov and N. Brosch, MNRAS **443**, 725 (2014).
[19] R. A. Perley and B. J. Butler, The Astrophysical Journal Supplement Series **230**, 7 (2017), 1609.05940.

Student: Trevor M. Oxholm
Advisor: Peter T. Timbie
Institution: University of Wisconsin-Madison
Year: 2

Abstract

The goal of my thesis research is to develop tools in radio interferometry and apply intensity-mapping techniques to early-universe neutral hydrogen (HI) lines. While a number of instruments are currently being developed with this goal, including HIRAX, CHIME, and the Tianlai Cylinder Array, my work revolves around the Tianlai dish array in Northwestern China. The Tianlai dish array features the unique advantage of being able to map redshifts ranging from 0 to 1.36 (600 MHz to 1420 MHz). If successful, the Tianlai Dish Array will use HI power spectra to constrain Baryon Acoustic Oscillations in the early universe, thus providing a powerful constraint on the dark energy equation of state. Furthermore, the technique will allow for unique and powerful three-dimensional mapping of the early universe.

Current Work

The Tianlai project is currently in its first stage, the *Pathfinder* stage. The goal of the stage is to accurately map the positions and redshifts of galaxies in the Northern hemisphere, before expanding the array in further stages. Much of my work has revolved around data analysis of recent radio surveys using the dish array. I have been developing systematic means of characterizing signals from the experiment's first runs on the North Celestial Pole, Cygnus A, and Cassiopeia A. Through systematic analysis of these measurements we are obtaining a deeper understanding of our instrument and developing analytical tools for the upcoming Polar Cap Survey.

Future Work/NRAO resources

As I develop systematic means to analyzing existing data runs, the Tianlai collaboration is preparing a Polar Cap Survey, as outlined in our GBT proposal. The main goal of the survey is to predict the redshifts of a sample of galaxies, which will be a powerful test for our instrument. The proposed GBT survey will be essential in accurately characterizing flux densities of the sample radio sources at the frequencies of interest for the Tianlai Pathfinder project. Furthermore, with these source maps we will be able to accurately calibrate the dishes and precisely measure characteristic beam patterns.

Degree Plan

The scientific goal of my thesis is to develop hands-on and data-analytical techniques in Hydrogen Intensity Mapping. I am entering my second year at University of Wisconsin-Madison, and the North Polar Cap Survey will be my first major undertaking as a graduate student. This survey marks an important milestone in the Tianlai Pathfinder stage, a crucial first step in developing a large Hydrogen Intensity Mapping array. Although the timeline of the Tianlai experiment extends beyond my likely tenure as a Ph.D. student, my work will be important as the collaboration pushes forward with more powerful data analytical techniques, and will provide valuable training as I begin my career in experimental cosmology.